Cardiovascular Revascularization Medicine 73 (2025) 50–58

Contents lists available at ScienceDirect

Cardiovascular Revascularization Medicine

journal homepage: www.sciencedirect.com/journal/cardiovascular-revascularization-medicine

Correcting common OCT artifacts enhances plaque classification and identification of higher-risk plaque features

Benn Jessney [a], Xu Chen [a], Sophie Gu [a], Adam Brown [b], Daniel Obaid [c], Charis Costopoulos [d], Martin Goddard [e], Nikunj Shah [f], Hector Garcia-Garcia [g], Yoshinobu Onuma [h,i], Patrick Serruys [i], Stephen P. Hoole [d], Michael Mahmoudi [j], Michael Roberts [a,k,l], Martin Bennett [a,l,*]

[a] Section of Cardiorespiratory Medicine, Department of Medicine, University of Cambridge, Cambridge, UK
[b] Monash Cardiovascular Research Centre, Monash University, Melbourne, Australia
[c] Swansea University Medical School and Morriston Regional Heart Centre, Swansea, UK
[d] Department of Cardiology, Royal Papworth Hospital, Cambridge, UK
[e] Department of Pathology, Royal Papworth Hospital, Cambridge, UK
[f] Department of Cardiology, Portsmouth Hospital, Portsmouth, UK
[g] Interventional Cardiology, MedStar Washington Hospital Center, DC, USA
[h] Galway University Hospital, Ireland
[i] Cardiovascular Research Centre for Advanced Imaging and Core Laboratory (CORRIB), University of Galway, Ireland
[j] Faculty of Medicine, University of Southampton, Southampton, UK
[k] Department of Applied Mathematics and Theoretical Physics, University of Cambridge, Cambridge, UK
[l] Octiocor Ltd, 201 Haverstock Hill, Second Floor Fkgb, London, UK

ARTICLE INFO

Keywords:
Atherosclerosis
Fibroatheroma
Optical coherence tomography
Artifact

ABSTRACT

Background: Optical coherence tomography (OCT) is used widely to guide stent placement, identify higher-risk plaques, and assess mechanisms of drug efficacy. However, a range of common artifacts can prevent accurate plaque classification and measurements, and limit usable frames in research studies. We determined whether pre-processing OCT images corrects artifacts and improves plaque classification.

Methods: We examined both *ex-vivo* and clinical trial OCT pullbacks for artifacts that prevented accurate tissue identification and/or plaque measurements. We developed Fourier transform-based software that reconstructed images free of common OCT artifacts, and compared corrected and uncorrected images.

Results: 48 % of OCT frames contained image artifacts, with 62 % of artifacts over or within lesions, preventing accurate measurement in 12 % frames. Pre-processing corrected >70 % of all artifacts, including thrombus, macrophage shadows, inadequate flushing, and gas bubbles. True tissue reconstruction was achieved in 63 % frames that would otherwise prevent accurate clinical measurements. Artifact correction was non-destructive and retained anatomical lumen and plaque parameters. Correction improved accuracy of plaque classification compared against histology and retained accurate assessment of higher-risk features. Correction also changed plaque classification and prevented artifact-related measurement errors in a clinical study, and reduced unmeasurable frames to <5 % *ex-vivo* and ~1 % *in-vivo*.

Conclusions: Fourier transform-based pre-processing corrects a wide range of common OCT artifacts, improving identification of higher-risk features and plaque classification, and allowing more of the whole dataset to be used for clinical decision-making and in research. Pre-processing can augment OCT image analysis systems both for stent optimization and in natural history or drug studies.

1. Introduction

Optical coherence tomography (OCT) is a high-resolution intravascular imaging modality that can help guide percutaneous coronary intervention (PCI) [1], monitor efficacy of anti-atherosclerosis drugs, and identify higher-risk features that predict major adverse cardiovascular events (MACE) [2–5]. However, real-world OCT frames frequently contain artifacts that limit their usefulness for stent optimization, cause

* Corresponding author at: Section of Cardiorespiratory Medicine, University of Cambridge, Victor Phillip Dardaleh Heart & Lung Research Institute, Papworth Road, Cambridge Biomedical Campus, Cambridge CB2 0BB, UK.
E-mail address: mrb24@cam.ac.uk (M. Bennett).

http://dx.doi.org/10.1016/j.carrev.2024.06.023
Received 2 May 2024; Received in revised form 19 June 2024; Accepted 28 June 2024
Available online 1 July 2024

misclassification of both tissues and plaques, and prevent measurement of higher-risk features [6,7]. Published consensus standards recommend measuring only good-quality images without artifacts [8], but this potentially excludes a large amount of clinical data. Artifacts may require additional pullbacks, analysis, and interpretation, introducing inter- and intra-observer variability, particularly by novice users [9].

We examined the range, frequency, and impact of artifacts from OCT acquisition and caused by different tissue types, and whether pre-processing images improves plaque characterization and number of frames analyzable frames.

2. Methods

2.1. Ex-vivo imaging and clinical trial datasets

A post-mortem *ex-vivo* dataset described previously ([10] and Supplemental Methods) along with consecutive DECODE study (NCT02335086) [11] patients that underwent OCT prior to culprit lesion PCI, and ASET-JAPAN [12] patients that underwent OCT as part of stent deployment in a study assessing prasugrel in chronic coronary syndromes was used to examine the range, frequency, and impact of OCT artifacts (Fig. 1A).

2.2. Artifact correction algorithm

After acquisition, OCT images were exported in Digital Imaging and Communications in Medicine (DICOM) format, before undergoing Fourier transform. The Fourier transform decomposes a spatial domain image into its sine and cosine components, with its output representing the image in the frequency domain, and number of frequencies corresponds to the number of pixels in the spatial domain image. In the Fourier domain, each point represents a particular frequency contained in the spatial domain image and is obtained by multiplying the spatial image with the corresponding base function (sine and cosine waves with increasing frequencies) and summing the result. In most implementations the Fourier

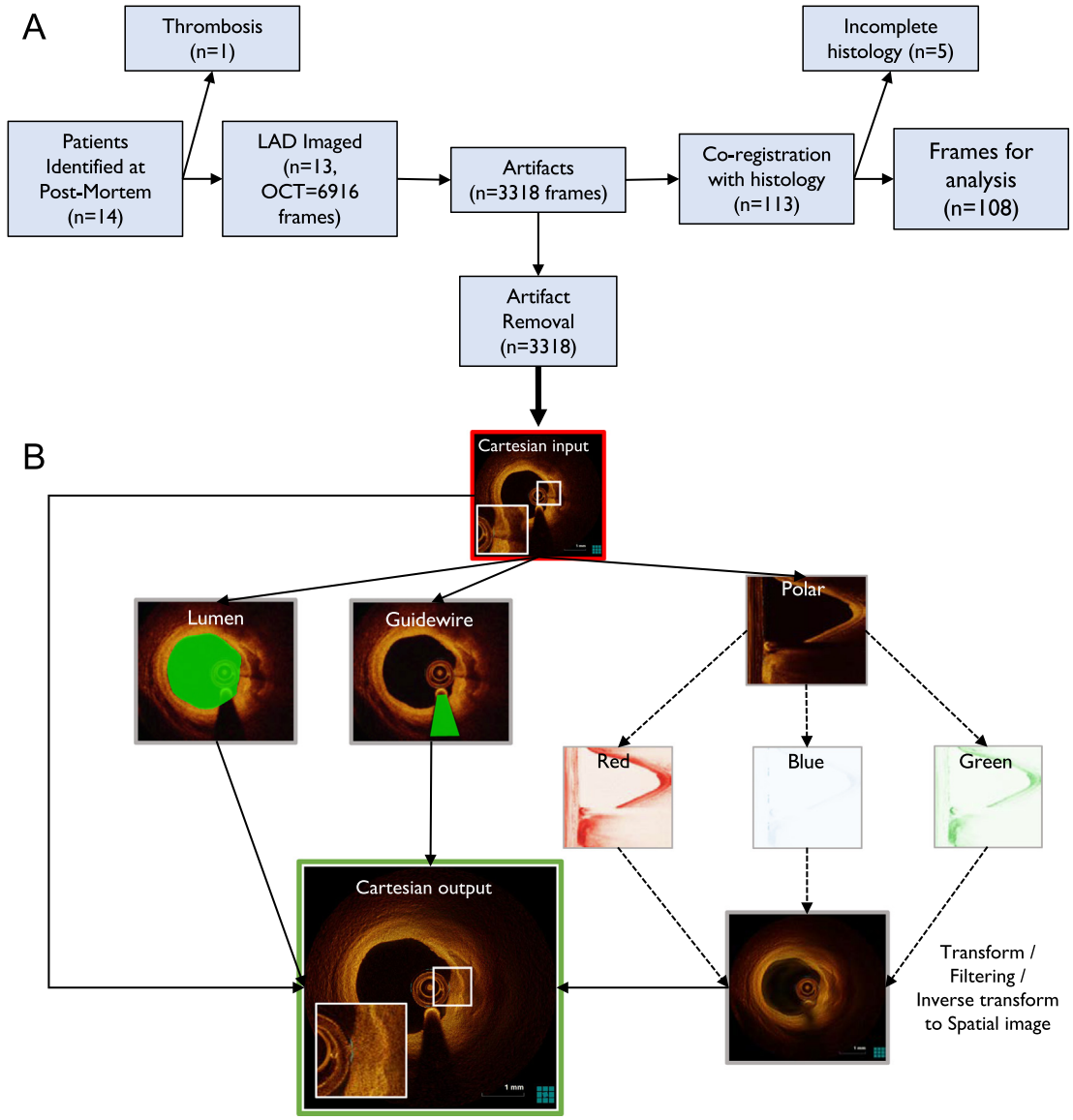

Fig. 1. Image processing software and study outline. **(A)** Schematic of *ex-vivo* study outline. 6916 OCT frames from 13 donors were assessed for artifacts, processed through the artifact removal software, and both corrected and uncorrected frames subsequently co-registered with histology. **(B)** Artifact removal. The original Cartesian OCT image was loaded, and vessel lumen and guidewire shadow detected utilizing a deep convolutional neural network. The Cartesian image was then converted to a polar image, before splitting into its RGB (red, green, blue) color channels. After Fourier transform filtering, and inverse transform, the image was reconstructed and merged with the original image, resulting in an artifact-free output image. 2.0× magnification images sampled from outlined areas.

image is shifted such that the image mean is displayed in the center of the image, with higher frequencies further from the center. Because Fourier domain images are decomposed into sinusoidal components, certain frequencies of the image may be processed, thus asserting an influence on the image when it is re-transformed to the spatial domain by the inverse Fourier transform.

Cartesian images were converted to polar orientation and split into component color channels before Fourier transform. In polar orientation, OCT artifacts appear at consistent points in the frequency domain. Frequency filtering was utilized to alter magnitude of artifact pixels such that image re-transformation resulted in artifact removal (Fig. 1B). Fourier transform of OCT images resulted in lumen and guidewire shadow processing artifacts, so these areas were detected *via* a Deep Convolutional Neural Network (Deeplabv3+) trained from manually segmented OCT pullbacks. Corrected OCT images displayed a smoothed appearance that could affect plaque characterization. The final artifact-free output image was therefore a blended filtered Fourier-transformed image with the original OCT image. Python 3.8 was used as the primary programming language with PyTorch 2.0 for the deep learning framework.

2.3. Plaque and tissue definitions and measurements

Exported OCT frames were processed and uncorrected and artifact-corrected OCT images compared offline using a LightLab Imaging workstation (St. Jude Medical) by an independent observer blinded to histology. Lumen contours and plaque composition were assessed. Plaques were classified following standard definitions ([6] and Supplemental Methods), lipid and calcium arc measurements recorded within each frame, and minimum FCT (fibrous cap thickness) measured at its thinnest part 3 times and mean value used. Histological sections and imaging data were measured in a random order.

2.4. Measurements & Statistical Analysis

Vessel lumen sizes are expressed in millimeters, tissue measurements in microns and arcs in degrees. Agreement between imaging or with histology was compared using the intraclass correlation coefficient (ICC) for absolute agreement, Bland–Altman plots to compare mean against difference in measurements, and Pearson's correlation coefficient with linear regression (r^2). Statistical significance threshold was set at 0.05. Statistical analyses were performed in SPSS 28.0.0 (SPSS Inc., IBM Computing).

3. Results

3.1. Frequency, range, and correction of ex-vivo artifacts

We first analyzed *ex-vivo* OCT pullbacks for artifacts, and then processed images for artifact correction before comparison with co-registered histology (Fig. 1). Fourteen post-mortem left anterior descending arteries were harvested and underwent OCT imaging under physiological pressures. Demographics are presented in **Table S1**. 6916 frames representing 1383 mm of coronary artery were analyzed up to the guide catheter and the most dominant artifact recorded. 48.0 % frames contained an artifact. An artifact was over or within a lesion in 62.7 % frames and prevented accurate clinical measurements in 853/6916 (12.3 %) frames (Fig. 2**, upper panel)**.

All frames underwent processing, with corrected deemed if the artifact was no longer visible or affected clinical measurements (Fig. 2**, lower panel)**. 70.4 % artifacts were corrected, with tissue reconstruction in 63 % frames that would otherwise prevent accurate clinical measurements, reducing overall unmeasurable frames to 4.6 %. Tissue reconstruction was achieved in all thrombus, macrophage shadow, superficial signal dropout, inadequate flushing, and gas bubble artifacts. Tangential signal dropout, seam and fold-over artifacts could not be corrected adequately by this method alone.

3.2. Artifact correction does not alter vessel size or shape and is non-detrimental to higher-risk plaque measurements

We next examined whether correction adversely affected important measurements for PCI and identification of higher-risk plaque features [8,13–16](Fig. 3). Corrected and uncorrected minimum (Fig. 3A) and maximum lumen diameters and lumen areas showed excellent agreement (ICC 0.98, $p < 0.01$; 0.97, $p < 0.01$; ICC 0.99 $p < 0.01$ respectively). Artifact corrected OCT-derived FCT measurements correlated better with histology-derived measurements (ICC 0.54, $p = 0.005$, *vs.* ICC 0.30, $p = 0.195$)(Fig. 3B). Uncorrected lipid arc measurements showed moderate correlation (ICC 0.55) but with proportional bias ($p = 0.02$), with larger measurements compared to histology (mean difference 22.65 *vs.* 8.86). Corrected lipid arcs also showed moderate correlation, but without proportional bias (ICC 0.52, $p = 0.009$), indicating that artifact correction does not adversely alter lipid arc measurements (Fig. 3C). Both uncorrected and corrected OCT-derived calcium arc correlated well with histology (ICC 0.87, $p = 0.002$ and 0.88, $p = 0.001$ respectively)(Fig. 3D).

3.3. Artifact correction improves classification of intimal thickening and fibroatheromas

We examined the effect of pre-processing on plaque classification in OCT frames containing artifacts co-registered with 108 histological sections (Table 1). Uncorrected-OCT plaque classification agreed with histological classification in only 56.5 % frames containing artifacts. Agreement was only 52.5 % for fibrous tissue (AIT or PIT) and 49.1 % for fibroatheroma frames, which improved to 75 % and 56.6 % respectively with correction (Table 1). Incorrectly identified fibroatheroma frames had more artifacts (27 *vs.* 4) and typically a thick fibrous cap or large fibrous tissue area (Fig. 4). Fibrocalcific lesions were accurately identified throughout.

The reported positive (PPV) and negative predictive (NPV) values and diagnostic accuracy of OCT for plaque classification against histology are variable [10,17–19] and potentially worse with artifacts. Artifact correction improved PPV, NPV and diagnostic accuracy for fibrous plaque, fibroatheroma and fibrocalcific plaque (Table 1). Correction also improved sensitivity and specificity of thin-cap fibroatheroma (TCFA, defined as FCT <65 μm) identification against histology whilst also improving PPV. Although correction reduced sensitivity to detect lipid arc >180 degrees, it increased specificity (Table 1).

3.4. Artifact correction reconstructs tissue in clinical OCT pullbacks

We next tested the effect of pre-processing in clinical trials using 2919 frames from 12 full OCT pullbacks from patients from the DECODE study (demographics are shown in **Table S2**). 69.3 % contained artifacts**.** Compared to *ex-vivo*, the clinical pullbacks contained proportionally more inadequate flushing and superficial signal dropout artifacts but fewer gas bubble, seam, tangential signal dropout, and thrombus artifacts. An artifact was over or within a lesion in 40.5 % frames, preventing accurate clinical measurements in 10.0 % frames (**Table S3**).

3.5. Artifact correction allows more clinical measurements and does not alter clinically important measurements in high-risk plaques

Pre-processing corrected 90.4 % artifacts in DECODE images. 291 artifacts prevented accurate clinical measurements, but tissue reconstruction was achieved in 244 frames. In contrast to *ex-vivo* pullbacks, only 72.9 % of thrombus artifacts were corrected, most likely as thrombus was larger *in-vivo* than *ex-vivo* and cast a large, dense shadow.

Artifact correction is particularly relevant to clinical trials, as TCFA and large lipid arcs predict MACE [8,13,14]. 11 TCFA comprising 116 frames were examined, of which 37.1 % contained an artifact, all of which prevented accurate measurements (**Table S3**). Reconstruction was achieved for all macrophage shadows, increasing measurable frames in TCFA by 74.4 %. Corrected FCT and lipid arc measurements

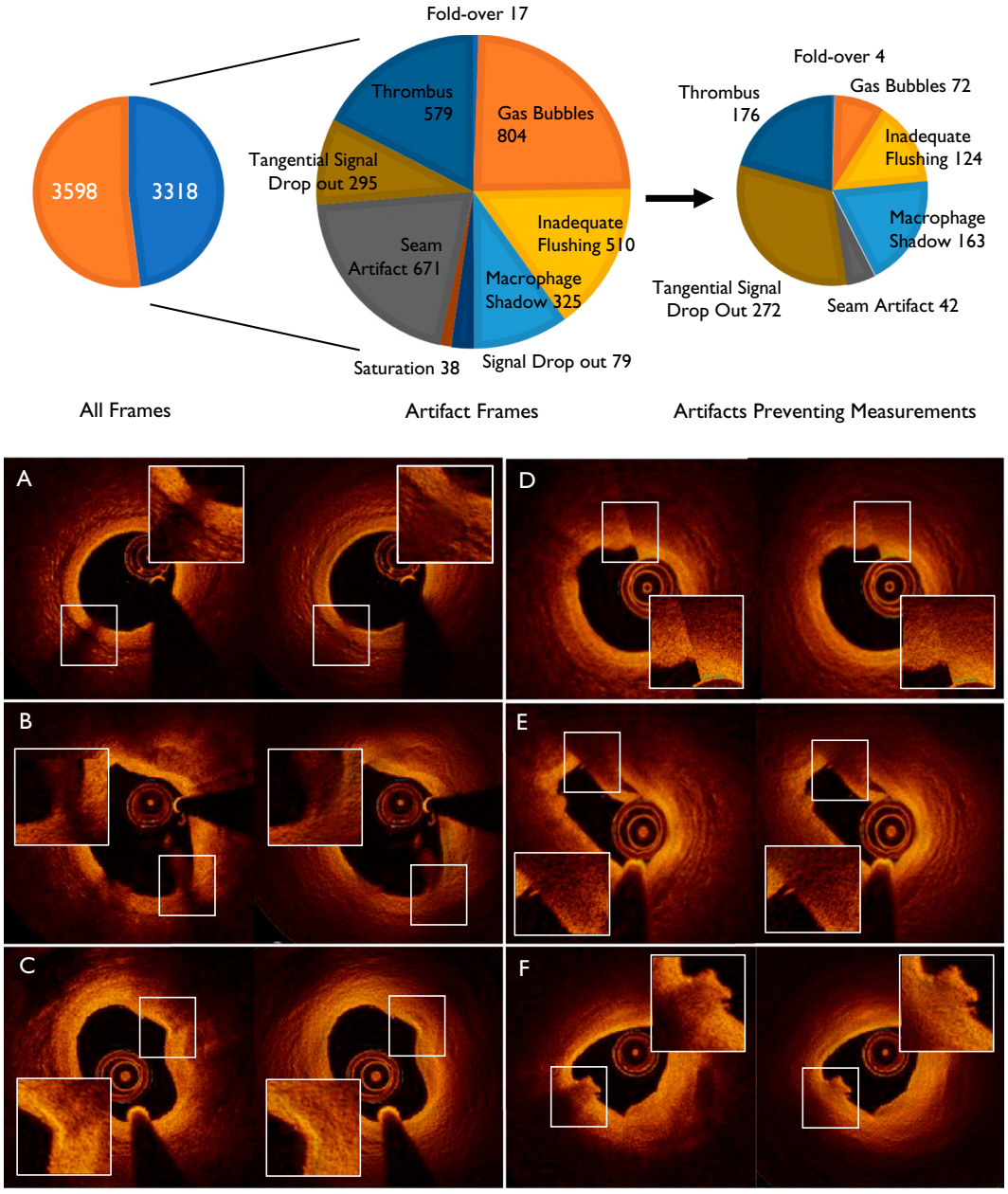

Fig. 2. Pre-processing corrects a wide range of OCT artifacts. Upper panel: The proportion and types of artifacts present *ex-vivo*. 3318/6916 frames (48.0 %) contained an artifact. 853/6916 frames contained artifacts which prevented accurate clinical measurements. Lower panel: uncorrected OCT image **(left)**, corrected image **(right)** showing artifacts due to **(A)** Gas Bubbles, **(B)** Inadequate Flushing, **(C)** Macrophage shadow, **(D)** Seam Artifact, **(E)** Tangential Signal Drop Out, **(F)** Thrombus. 2.0× magnification images are sampled from outlined areas.

correlated well with uncorrected measurements in TCFAs (ICC 0.75, $p \leq 0.001$ and ICC 0.99, $p \leq 0.001$ respectively), indicating that artifact correction in TCFAs does not adversely alter clinically important measurements **(**Fig. 5**)**.

3.6. Imaging artifacts in modern OCT-systems

To exclude the possibility that newer OCT catheters and technology negate need for artifact correction, we also analyzed 10 pullbacks representing 659 mm of coronary artery from randomly selected patients from the ASET-JAPAN study [12]. Although ASET-JAPAN pullbacks contained fewer artifacts that prevented accurate clinical measurements, the incidence and range of artifacts was similar with newer C8-XRTM or OPTISTM compared to older C7 catheters (Abbott Vascular, Santa Clara, CA, USA) (**Table S4**).

4. Discussion

We find that **(a)** Post-mortem and clinical OCT pullbacks contain a similar and wide range of artifacts; **(b)** Artifacts were present in ~50 % of frames at post-mortem, 62.7 % over or within a plaque, and 12.3 % prevented accurate measurement of plaque features; **(c)** Artifacts were present in 69.3 % of clinical OCT pullbacks, over or within a lesion in 40.5 %, and prevented accurate clinical measurements in 10.0 %; **(d)** Image pre-processing corrected >70 % of artifacts, including all macrophage shadow, inadequate flushing, and gas bubble artifacts, and most thrombus artifacts; **(e)** Pre-processing reduced unmeasurable frames to <5 % *ex-vivo* and ~ 1 % *in-vivo*; **(f)** Pre-processing improved accuracy of fibrous plaque and fibroatheroma detection *vs.* histology, and did not affect lumen measurements or higher risk features such as FCT or lipid arcs; **(g)** Correction changed plaque classification and

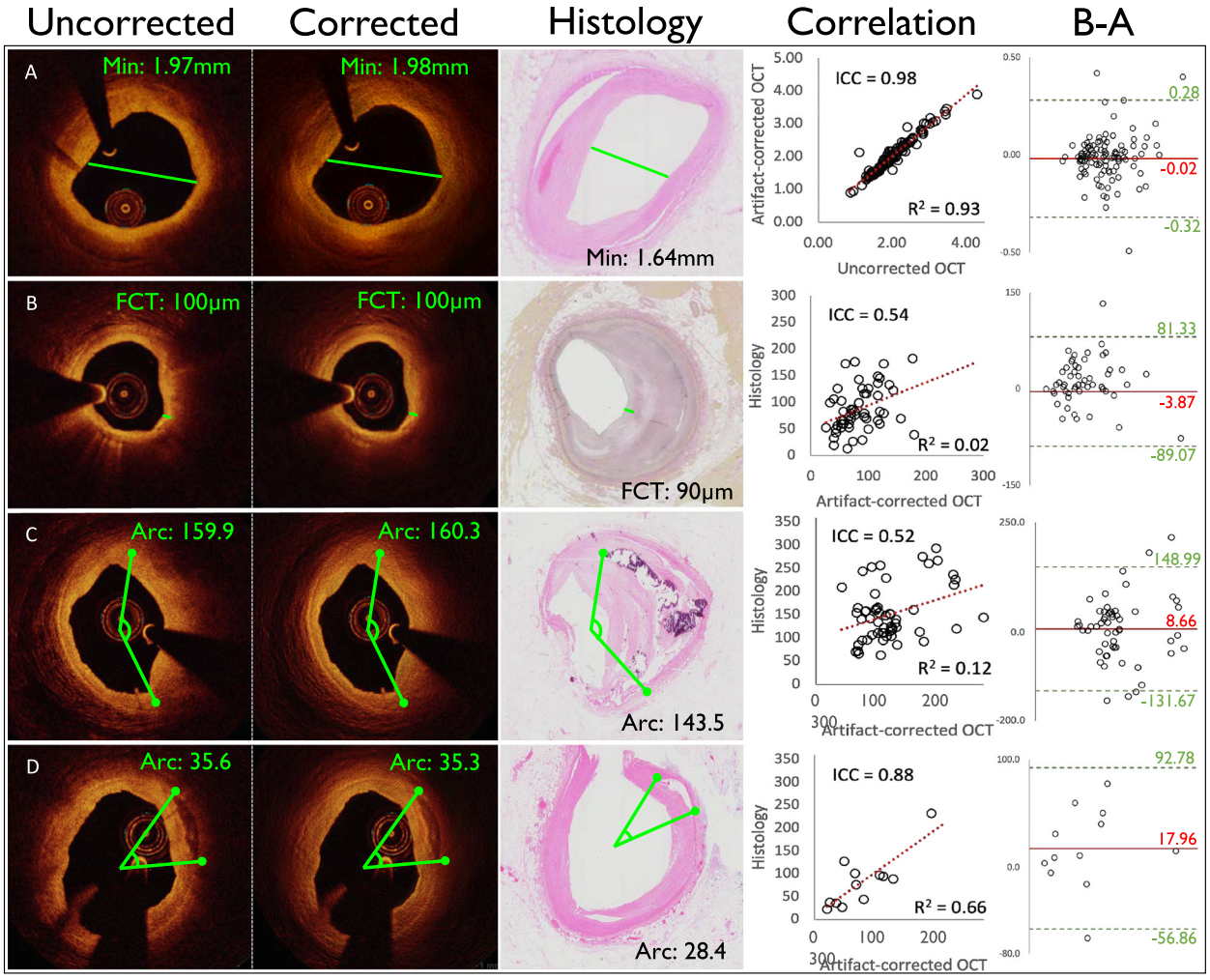

Fig. 3. Artifact correction does not alter vessel size or shape and is non-detrimental to measurement of higher-risk plaque features. Comparison of measurements taken on (left to right) uncorrected-OCT, artifact-corrected OCT, and co-registered histology section; with both correlation plot and Bland-Altman (B-A) showing agreement between measurements. Intraclass correlation coefficient (ICC) and R^2 are shown. **(A)** Comparison of minimum lumen diameter measurements; with agreement between minimum lumen diameter measurements taken on uncorrected and artifact-corrected OCT images shown. **(B)** FCT measured. Correlation plot and B-A plot showing agreement between FCT measured on artifact-corrected OCT images and histology. **(C)** Lipid arc measured; with correlation plot and B-A analysis showing agreement between corrected OCT images and histology. **(D)** Calcium arc measured; with correlation plot and B-A analysis showing agreement between corrected OCT images and histology. Upper and lower 95 % confidence intervals (green) and average difference (red) are shown for all Bland-Altman plots.

Table 1
Accuracy of uncorrected-OCT and artifact-corrected OCT plaque classification, TCFA classification, and identification of higher-risk plaque features compared with histology.

Uncorrected-OCT	Histological classification					
	Normal (n = 3)	Fibrous (AIT/PIT) (n = 40)	FA (n = 53)	Fibrocalcific (n = 12)	TCFA (n = 21)	Lipid Arc > 180° (n = 14)
Uncorrected-OCT						
Correctly Identified (n)	2/3	21/40	26/53	12/12	7/21	10/14
Sensitivity (%)	66.7	70.0	49.1	100.0	33.3	71.4
Specificity (%)	93.3	86.8	81.8	78.1	86.2	81.4
PPV (%)	22.2	69.0	72.2	36.4	45.4	36.4
NPV (%)	99.0	75.5	62.5	100	79.0	95.0
Diagnostic Accuracy (%)	92.6	73.3	65.7	80.6	75.9	79.0
Artifact-corrected OCT						
Correctly Identified (n)	3/3	30/40	30/53	12/12	10/21	7/14
Sensitivity (%)	100.0	75.0	56.6	100.0	52.4	53.9
Specificity (%)	95.2	86.8	92.7	84.4	89.8	88.1
PPV (%)	37.5	76.9	88.2	44.4	63.9	40.2
NPV (%)	100	85.5	68.9	100.0	84.6	92.8
Diagnostic Accuracy (%)	95.4	82.4	75.0	86.1	80.0	80.0

Estimates of diagnostic performance. Fibrous includes AIT and PIT; FA, fibroatheroma; TCFA, Thin-cap fibroatheroma; NPV, negative predictive value; PPV, positive predictive value.

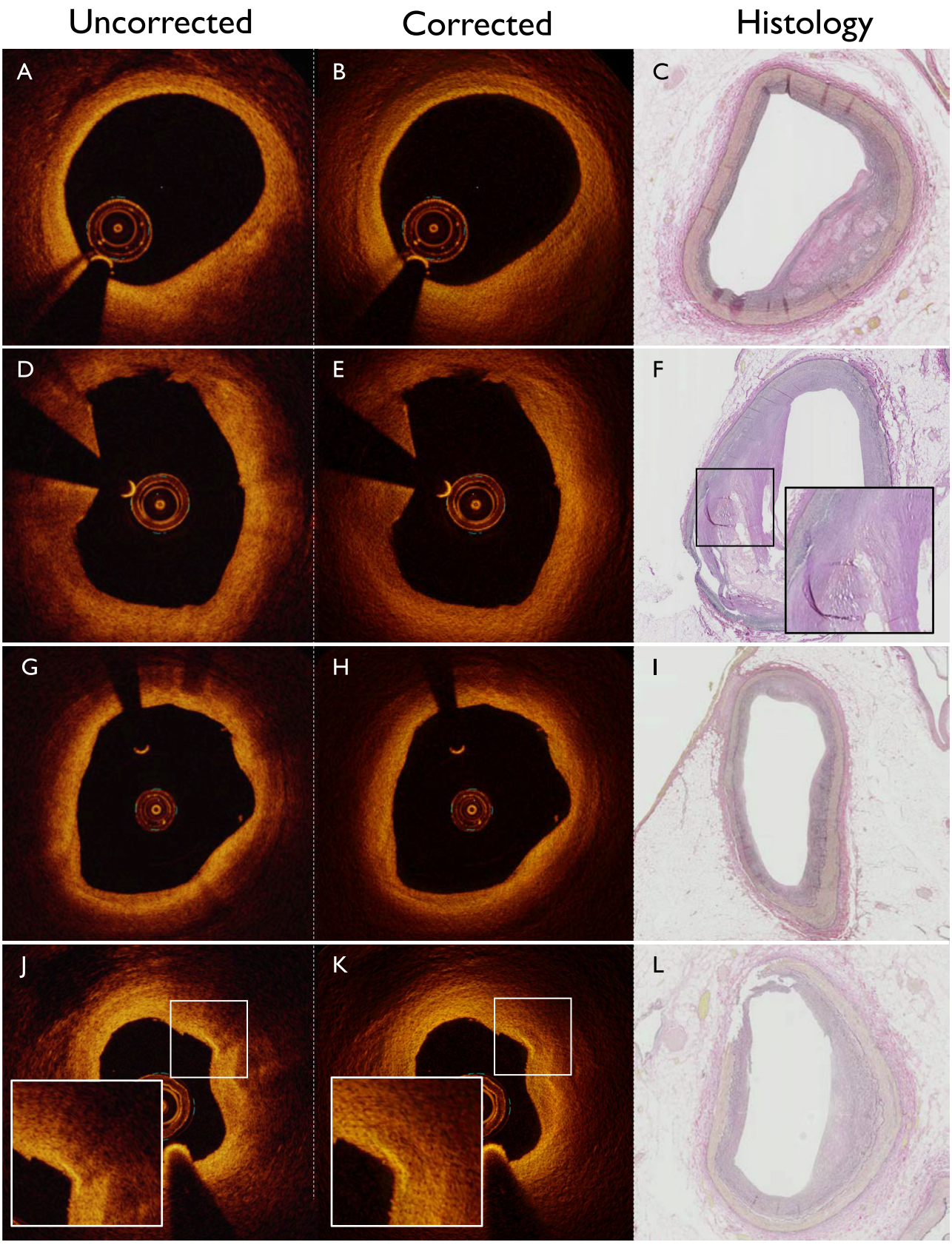

(caption on next page)

prevented artifact-related measurement errors in clinical OCT pullbacks, including for TCFAs.

Consensus standards recommend using only good-quality OCT images without artifacts for measurements [8]. However, the true OCT artifact burden is unknown with reports up to 11.2 % unusable frames [20], or studies have strict eligibility criteria that include a continuous arc of at least 270 degrees around the lumen center and qualitative definition of superficial plaque components [14], both of which limit analyzable frames. Similarly, we find artifacts prevented accurate clinical assessment in 10.0 % of OCT frames. Artifacts also cause clinical misinterpretation, with tangential signal dropout and signal attenuation leading to signal-poor areas being mistaken for lipid-rich regions [6]. While inter- and intra-observer variability is low for OCT in highly experienced, high-volume operators [21], inexperienced users have significantly worse plaque assessment *via* OCT [9], and variability may be higher in real-time analysis where artifacts may not be recognized.

We demonstrate that *ex-vivo* OCT pullbacks demonstrate a large range of artifacts affecting accurate measurement of plaque features. Published studies report high accuracy of *ex-vivo* OCT to identify plaque tissues [22,23] and classification [24,25]. We find that although accuracy to detect normal tissue was high, the ability of uncorrected-OCT to identify fibrous plaques and fibroatheroma was lower (73.3 % and 65.7 % respectively). Artifacts preventing accurate classification were commonly due to shadows on surrounding tissue or light absorption. For example, macrophages causing superficial shadowing that resembles lipid-rich plaque or thin-cap fibroatheromas. In contrast, pre-processing improved sensitivity and diagnostic accuracy to detect fibrous plaques and fibroatheroma.

Thin fibrous caps and large lipid arcs are prognostic features for future MACE. However, while FCT detected by OCT and histology show good correlation and diagnostic accuracy [25], the reported positive predictive value of OCT for TCFA identification against histology varies between 37 and 41 % [17,26] which may partly explain the very different incidence of TCFA in OCT studies *vs.* histology (1.6 % *vs.* 6.9 % in non-ACS and 44.4 % in ACS plaques) [17–19]. Reasons for this include strong scattering and attenuation of near infra-red light and attenuation by large lipid cores [17] and artifacts that affect measurement accuracy. FCT and lipid arc measurements require high accuracies, as thin caps are defined in microns, and whilst the reported changes are greater with drugs such as Evolocumab [27], drugs that reduce MACE such as high-intensity statins increase FCT by only ~20 μm and decrease lipid arc by only 12.4 degrees in some studies [28,29].

In addition to plaque classification, a minimal lumen area (MLA) $<3.5mm^2$, high plaque burden, small FCT, and large lipid arc are associated with increased MACE [13,30]. As well as providing accurate vessel sizing, OCT also helps identify suitable landing zones for PCI that avoid calcium-rich areas, or assessing calcification that may require adjunctive treatments. Image pre-processing did not alter lumen area, and maximum and minimum lumen diameters *ex-vivo* or in clinical studies, or the accuracy of FCT or lipid arc measurements *vs.* histology, indicating that artifact correction does not alter clinically important plaque or coronary lumen measurements.

Our work has some limitations. First, the post-mortem study examined 13 OCT pullbacks and findings should be validated in larger data sets; however, 108 OCT frames with 108 ROI were co-registered with histology from the entire pullback rather than just specific plaque types, suggesting a robust applicability to clinical OCT. Second, the range and frequency of artifacts may vary in different clinical studies *vs. ex-vivo*. However, prevalence of artifacts that affect tissue type identification, plaque classification, and measurements was similar between *ex-vivo* and *in-vivo* datasets, even with newer catheters. Third, the clinical OCT analysis does not define the true incidence of TCFA, and artifacts from tangential signal dropout or macrophage shadows may mimic TCFAs on OCT. However, although our pre-processing could not restore fold-over, seam and tangential signal dropout artifacts, it significantly improved sensitivity and accuracy of tissue type detection and plaque classification. Finally, co-registration between OCT and histology is challenging and small longitudinal mismatches may influence correlations of measurements. However, an experienced imaging specialist performed all co-registration blinded to plaque classification, and there was a good correlation between both corrected and uncorrected FCT and lipid arc between OCT and histology.

5. Conclusion

We find a high frequency of artifacts in OCT images from clinical datasets, including over or within lesions that prevent accurate measurements. Fourier transform-based pre-processing corrects a wide range of common OCT artifacts, improving identification of higher-risk features and plaque classification, and allowing more of the whole dataset to be used for clinical decision-making and in research. We conclude that image preprocessing may be a useful adjunct to OCT image analysis.

Funding

This work was supported by British Heart Foundation Grants FS/19/66/34658, RG71070, RG84554, BHF Cambridge Centre for Research Excellence, EPSRC Cambridge Maths in Healthcare Centre Nr. EP/N014588/1, and Cambridge NIHR Biomedical Research Centre.

CRediT authorship contribution statement

Benn Jessney: Writing – review & editing, Writing – original draft, Visualization, Software, Project administration, Methodology, Investigation, Formal analysis, Data curation, Conceptualization. **Xu Chen:** Writing – review & editing, Software, Investigation. **Sophie Gu:** Writing – review & editing, Investigation, Data curation. **Adam Brown:** Writing – review & editing, Investigation, Data curation. **Daniel Obaid:** Writing – review & editing, Investigation, Data curation. **Charis Costopoulos:** Writing – review & editing, Investigation, Data curation. **Martin Goddard:** Writing – review & editing, Investigation, Data curation. **Nikunj Shah:** Writing – review & editing, Investigation, Data curation. **Hector Garcia-Garcia:** Writing – review & editing, Investigation, Data curation. **Yoshinobu Onuma:** Writing – review & editing, Investigation, Data curation. **Patrick Serruys:** Writing – review & editing, Investigation, Data curation. **Stephen P. Hoole:** Writing – review & editing, Investigation, Data curation. **Michael Mahmoudi:** Writing – review & editing, Investigation, Data curation. **Michael Roberts:** Writing – review & editing, Validation, Software, Formal analysis. **Martin Bennett:** Writing – review & editing, Writing – original draft, Visualization, Validation, Supervision, Resources, Project administration, Funding acquisition, Formal analysis.

Declaration of competing interest

MR and MRB are founders of Octiocor Ltd., a software imaging company.

Fig. 4. Correctly and incorrectly OCT-classified fibroatheroma and fibrous tissue examples. **(A-C)** Fibroatheroma correctly classified by both uncorrected and corrected OCT with corresponding co-registered histology section. **(D—F)** Example of an incorrectly identified fibroatheroma on both uncorrected and corrected OCT. A thick fibrous cap with dense fibrous tissue is seen **(F)**. **(G-I)** Adaptive intimal thickening correctly identified by uncorrected and corrected OCT, seen as loss of tri-layer appearance of normal tissue and intimal thickening. **(J-L)** Example of incorrectly identified section of pathological intimal thickening. Uncorrected-OCT shows a signal-poor region with poorly defined borders and fast OCT signal drop-off classified as a fibroatheroma **(J)**. Corrected OCT displays a more homogenous lesion with limited signal attenuation classified as fibrous plaque **(K)**. 2.0× magnification images sampled from outlined areas.

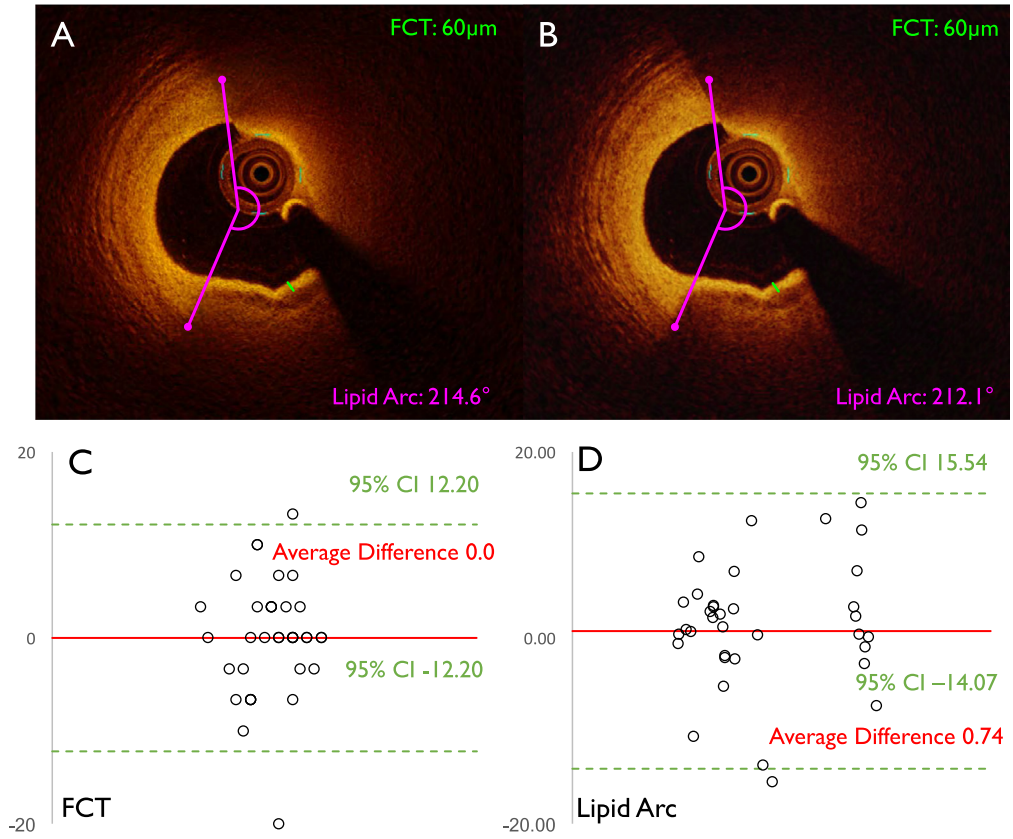

Fig. 5. Artifact correction does not alter measurements of FCT or lipid arc at sites of TCFA. **(A-B)** Fibrous cap thickness and lipid arc measured on artifact-corrected OCT images **(A)** and uncorrected images **(B)**. **(C)** Bland-Altman plot of FCT measurements on corrected *vs.* uncorrected-OCT images. **(D)** Bland-Altman plot of lipid arc measurements on corrected-OCT images compared with uncorrected-OCT images. Statistically similar correlations are seen with both clinical parameters. 95 % confidence intervals (CI) are shown.

Appendix A. Supplementary data

Supplementary data to this article can be found online at https://doi.org/10.1016/j.carrev.2024.06.023.

References

[1] Ali ZA, Maehara A, Genereux P, Shlofmitz RA, Fabbiocchi F, Nazif TM, et al. Optical coherence tomography compared with intravascular ultrasound and with angiography to guide coronary stent implantation (ILUMIEN III: OPTIMIZE PCI): a randomised controlled trial. Lancet. 2016;388(10060):2618–28. https://doi.org/10.1016/S0140-6736(16)31922-5.

[2] Narula J, Nakano M, Virmani R, Kolodgie FD, Petersen R, Newcomb R, et al. Histopathologic characteristics of atherosclerotic coronary disease and implications of the findings for the invasive and noninvasive detection of vulnerable plaques. J Am Coll Cardiol. 2013;61(10):1041–51. https://doi.org/10.1016/j.jacc.2012.10.054.

[3] Kubo T, Ino Y, Mintz GS, Shiono Y, Shimamura K, Takahata M, et al. Optical coherence tomography detection of vulnerable plaques at high risk of developing acute coronary syndrome. Eur Heart J Cardiovasc Imaging. 2021. https://doi.org/10.1093/ehjci/jeab028.

[4] Mizukoshi M, Kubo T, Takarada S, Kitabata H, Ino Y, Tanimoto T, et al. Coronary superficial and spotty calcium deposits in culprit coronary lesions of acute coronary syndrome as determined by optical coherence tomography. Am J Cardiol. 2013;112(1):34–40. https://doi.org/10.1016/j.amjcard.2013.02.048.

[5] Prati F, Gatto L, Romagnoli E, Limbruno U, Fineschi M, Marco V, et al. In vivo vulnerability grading system of plaques causing acute coronary syndromes: an intravascular imaging study. Int J Cardiol. 2018;269:350–5. https://doi.org/10.1016/j.ijcard.2018.06.115.

[6] van Soest G, Regar E, Goderie TP, Gonzalo N, Koljenovic S, van Leenders GJ, et al. Pitfalls in plaque characterization by OCT: image artifacts in native coronary arteries. JACC Cardiovasc Imaging. 2011;4(7):810–3. https://doi.org/10.1016/j.jcmg.2011.01.022.

[7] Araki M, Park SJ, Dauerman HL, Uemura S, Kim JS, Di Mario C, et al. Optical coherence tomography in coronary atherosclerosis assessment and intervention. Nat Rev Cardiol. 2022. https://doi.org/10.1038/s41569-022-00687-9.

[8] Tearney GJ, Regar E, Akasaka T, Adriaenssens T, Barlis P, Bezerra HG, et al. Consensus standards for acquisition, measurement, and reporting of intravascular optical coherence tomography studies: a report from the International Working Group for Intravascular Optical Coherence Tomography Standardization and Validation. J Am Coll Cardiol. 2012;59(12):1058–72. https://doi.org/10.1016/j.jacc.2011.09.079.

[9] Martin WG, McNaughton E, Bambrough PB, West NEJ, Hoole SP. Interobserver variability between expert, experienced and novice operator affects interpretation of optical coherence tomography & 20 MHz intravascular ultrasound imaging. Cardiovasc Revasc Med. 2022. https://doi.org/10.1016/j.carrev.2022.09.021.

[10] Brown AJ, Obaid DR, Costopoulos C, Parker RA, Calvert PA, Teng Z, et al. Direct comparison of virtual-histology intravascular ultrasound and optical coherence tomography imaging for identification of thin-cap fibroatheroma. Circ Cardiovasc Imaging. 2015;8(10):e003487. https://doi.org/10.1161/CIRCIMAGING.115.003487.

[11] Shah N, Meira LB, Elliott RM, Hoole SP, West NE, Brown AJ, et al. DNA damage and repair in patients with coronary artery disease: correlation with plaque morphology using optical coherence tomography (DECODE study). Cardiovasc Revasc Med. 2019;20(9):812–8. https://doi.org/10.1016/j.carrev.2019.04.028.

[12] Muramatsu T, Masuda S, Kotoku N, Kozuma K, Kawashima H, Ishibashi Y, et al. Prasugrel monotherapy after percutaneous coronary intervention with biodegradable-polymer platinum-chromium Everolimus eluting stent for Japanese patients with chronic coronary syndrome (ASET-JAPAN). Circ J. 2023;87(6):857–65. https://doi.org/10.1253/circj.CJ-23-0051.

[13] Xing L, Higuma T, Wang Z, Aguirre AD, Mizuno K, Takano M, et al. Clinical significance of lipid-rich plaque detected by optical coherence tomography: a 4-year follow-up study. J Am Coll Cardiol. 2017;69(20):2502–13. https://doi.org/10.1016/j.jacc.2017.03.556.

[14] Prati F, Romagnoli E, Gatto L, La Manna A, Burzotta F, Ozaki Y, et al. Relationship between coronary plaque morphology of the left anterior descending artery and 12 months clinical outcome: the CLIMA study. Eur Heart J. 2020;41(3):383–91. https://doi.org/10.1093/eurheartj/ehz520.

[15] Raber L, Mintz GS, Koskinas KC, Johnson TW, Holm NR, Onuma Y, et al. Clinical use of intracoronary imaging. Part 1: guidance and optimization of coronary interventions. An expert consensus document of the European Association of Percutaneous Cardiovascular Interventions. Eur Heart J. 2018;39(35):3281–300. https://doi.org/10.1093/eurheartj/ehy285.

[16] Fujino A, Mintz GS, Matsumura M, Lee T, Kim SY, Hoshino M, et al. A new optical coherence tomography-based calcium scoring system to predict stent underexpansion. EuroIntervention. 2018;13(18). https://doi.org/10.4244/EIJ-D-17-00962. e2182-e9.

[17] Fujii K, Hao H, Shibuya M, Imanaka T, Fukunaga M, Miki K, et al. Accuracy of OCT, grayscale IVUS, and their combination for the diagnosis of coronary TCFA: an ex vivo validation study. JACC Cardiovasc Imaging. 2015;8(4):451–60. https://doi.org/10.1016/j.jcmg.2014.10.015.

[18] Kato K, Yonetsu T, Kim SJ, Xing L, Lee H, McNulty I, et al. Nonculprit plaques in patients with acute coronary syndromes have more vulnerable features compared with those with non-acute coronary syndromes: a 3-vessel optical coherence tomography study. Circ Cardiovasc Imaging. 2012;5(4):433–40. https://doi.org/10.1161/CIRCIMAGING.112.973701.
[19] Cheruvu PK, Finn AV, Gardner C, Caplan J, Goldstein J, Stone GW, et al. Frequency and distribution of thin-cap fibroatheroma and ruptured plaques in human coronary arteries: a pathologic study. J Am Coll Cardiol. 2007;50(10):940–9. https://doi.org/10.1016/j.jacc.2007.04.086.
[20] Motreff P, Levesque S, Souteyrand G, Sarry L, Ouchchane L, Citron B, et al. High-resolution coronary imaging by optical coherence tomography: feasibility, pitfalls and artefact analysis. Arch Cardiovasc Dis. 2010;103(4):215–26. https://doi.org/10.1016/j.acvd.2010.03.002.
[21] Gerbaud E, Weisz G, Tanaka A, Kashiwagi M, Shimizu T, Wang L, et al. Multi-laboratory inter-institute reproducibility study of IVOCT and IVUS assessments using published consensus document definitions. Eur Heart J Cardiovasc Imaging. 2016;17(7):756–64. https://doi.org/10.1093/ehjci/jev229.
[22] Tearney GJ, Brezinski ME, Bouma BE, Boppart SA, Pitris C, Southern JF, et al. In vivo endoscopic optical biopsy with optical coherence tomography. Science. 1997;276(5321):2037–9. https://doi.org/10.1126/science.276.5321.2037.
[23] Yabushita H, Bouma BE, Houser SL, Aretz HT, Jang IK, Schlendorf KH, et al. Characterization of human atherosclerosis by optical coherence tomography. Circulation. 2002;106(13):1640–5. https://doi.org/10.1161/01.cir.0000029927.92825.f6.
[24] Kume T, Akasaka T, Kawamoto T, Watanabe N, Toyota E, Neishi Y, et al. Assessment of coronary arterial plaque by optical coherence tomography. Am J Cardiol. 2006;97(8):1172–5. https://doi.org/10.1016/j.amjcard.2005.11.035.
[25] Kume T, Akasaka T, Kawamoto T, Okura H, Watanabe N, Toyota E, et al. Measurement of the thickness of the fibrous cap by optical coherence tomography. Am Heart J. 2006;152(4):755:e1–4. https://doi.org/10.1016/j.ahj.2006.06.030.
[26] Phipps JE, Hoyt T, Vela D, Wang T, Michalek JE, Buja LM, et al. Diagnosis of thin-capped Fibroatheromas in intravascular optical coherence tomography images: effects of light scattering. Circ Cardiovasc Interv. 2016;9(7). https://doi.org/10.1161/CIRCINTERVENTIONS.115.003163.
[27] Nicholls SJ, Kataoka Y, Nissen SE, Prati F, Windecker S, Puri R, et al. Effect of Evolocumab on coronary plaque phenotype and burden in statin-treated patients following myocardial infarction. JACC Cardiovasc Imaging. 2022;15(7):1308–21. https://doi.org/10.1016/j.jcmg.2022.03.002.
[28] Raber L, Koskinas KC, Yamaji K, Taniwaki M, Roffi M, Holmvang L, et al. Changes in coronary plaque composition in patients with acute myocardial infarction treated with high-intensity statin therapy (IBIS-4): a serial optical coherence tomography study. JACC Cardiovasc Imaging. 2019;12(8 Pt 1):1518–28. https://doi.org/10.1016/j.jcmg.2018.08.024.
[29] Nishiguchi T, Kubo T, Tanimoto T, Ino Y, Matsuo Y, Yamano T, et al. Effect of early pitavastatin therapy on coronary fibrous-cap thickness assessed by optical coherence tomography in patients with acute coronary syndrome: the ESCORT study. JACC Cardiovasc Imaging. 2018;11(6):829–38. https://doi.org/10.1016/j.jcmg.2017.07.011.
[30] Wang Y, Zhao X, Zhou P, Liu C, Liao Z, Wang X, et al. High-risk culprit plaque predicts cardiovascular outcomes independently of plaque rupture in ST-segment elevation myocardial infarction: insight from optical coherence tomography. Angiology. 2022:33197221087778. https://doi.org/10.1177/00033197221087778.